Science of the Total Environment 770 (2021) 144741

Contents lists available at ScienceDirect

Science of the Total Environment

journal homepage: www.elsevier.com/locate/scitotenv

Future projections of water level and thermal regime changes of a multipurpose subtropical reservoir (Sao Paulo, Brazil)

Carolina Cerqueira Barbosa [a,*], Maria do Carmo Calijuri [a], André Cordeiro Alves dos Santos [b], Robert Ladwig [c], Lais Ferrer Amorim de Oliveira [d], Ana Carolina Sarmento Buarque [a]

[a] Hydraulics and Sanitation Department, University of São Paulo at São Carlos School of Engineering, São Carlos, SP, Brazil
[b] Biology Department, University of São Carlos-Sorocaba, Sorocaba, SP, Brazil
[c] Center for Limnology, University of Wisconsin-Madison, Madison, WI, USA
[d] Department of Civil Engineering, Polytechnic School, University of São Paulo, São Paulo, SP, Brazil

HIGHLIGHTS

- Regionalized climate model projections were used to assess water level and water temperature changes.
- Drought periods associated with a drop in water level led to a short-term decrease in the reservoir stratification.
- RCP 4.5 and RCP 8.5 climate scenarios will lead to the reservoir dead storage by the end of 2020s
- The heating of surface water layers and intensification of thermal stability can become a potential water quality issue.

GRAPHICAL ABSTRACT

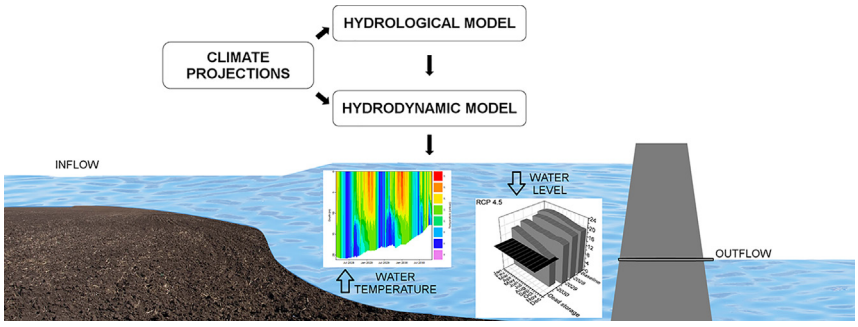

ARTICLE INFO

Article history:
Received 11 September 2020
Received in revised form 5 November 2020
Accepted 22 December 2020
Available online 23 January 2021

Editor: Martin Drews

Keywords:
Lake modeling
General Lake Model (GLM)
Itupararanga reservoir
Climate projections

ABSTRACT

The increase in global air temperatures as well as variability in rainfall shifts due to climate change has been affecting the dynamics of water level fluctuations and thermal regimes in lakes and reservoirs. It is expected that at the end of this decade, such impacts will be even more noticeable and may harm the inland waters use. However, little is known about the possible consequences of climate change in multipurpose subtropical reservoirs. Using data generated by a regionalized climate model (RCM) as input to a simple hydrological model and a one-dimensional vertical hydrodynamic model, we forecast potential changes in the Itupararanga reservoir, São Paulo, Brazil, in an exemplary time period (2028–2030) in the next decade. Two Representative Concentration Pathway (RCP) scenarios were considered: an optimistic one corresponding to a CO_2 increase of about 650 ppm (RCP 4.5) and a pessimistic scenario where CO_2 exceeds 1000 ppm in 2100 (RCP 8.5). We found a significant reduction in the reservoir water level for both scenarios of 35% compared to current conditions. The surface water temperature is expected to increase (+0.6 °C); on the other hand, there would be a cooling of the hypolimnion (RCP 4.5 =-0.3 °C; RCP 8.5 = −1.2 °C). Another consequence is an increase of the duration of stratification periods that would start earlier in the dry period (between July and August), as well as the intensification of the stability of the water column (+43% compared to current conditions) and a deepening of the thermocline. The hydrodynamic modeling results suggest that the water level drop may threaten the reservoir multiple uses, in particular drinking water supply and power generation. Furthermore, the heating of surface water layers and increase of the number of stratified days and thermal stability can have negative impacts on water quality.

* Corresponding author.
E-mail address: carolina.cbarbosa@usp.br (C.C. Barbosa).

https://doi.org/10.1016/j.scitotenv.2020.144741
0048-9697/

1. Introduction

Sustainable development goals have assumed a new paradigm with Earth's life-support system, society, and economy including targets for 2030 (Griggs et al., 2013). Concerns about clean water, as well as the health and production of ecosystems are intrinsically linked to climate change.

Some of the consequences of climate change are a rise in air temperatures and alterations in rainfall patterns (IPCC, 2014). The water levels of lakes and reservoirs have shifted due to the increase in the frequency of occurrence of weather extremes. More frequent drought and flood periods have been reported worldwide (Brasil et al., 2016; Soares et al., 2019; Jeppesen et al., 2015). Scientific research has focused on a relationship between volume fluctuations and water quality degradation, in particular the nutrients dynamics, trophic state, and phytoplankton community (Jeppesen et al., 2015).

There is also evidence that climate change influences the thermal dynamics of inland waters (Sahoo et al., 2016). The air temperature increase has been reported as a driver of heating surface water temperature (Zhang et al., 2020) and another consequence are alterations in the heat budgets of lakes (Woolway and Merchant, 2019). All of those alterations can lead to cyanobacteria dominance (Kosten et al., 2012) and blooms (Wells et al., 2015; Huisman et al., 2018).

In this way, global and regionalized climate models have been applied under different concentration pathway scenarios to predict climate change impacts (Eccles et al., 2019; Fenocchi et al., 2018; Prats et al., 2018). Using this forecast data has enabled a better understanding of the global warming effects on aquatic ecosystems. Especially coupling climate models to aquatic ecosystem models has been used to predict the consequences of climate change on aquatic environments (Moe et al., 2016). Furthermore, these coupled models are used to test adaptive water management measures for the potential mitigation of negative impacts on the ecosystem (Ladwig et al., 2018).

Climate change effects have already been highlighted in global lake ecosystems (Jeppesen et al., 2017; Woolway and Merchant, 2019). However, further studies are needed to incorporate the likely impacts of climate change in vulnerability assessments and lake management efforts (O'Reilly et al., 2015). Although a water temperature increase is prospective to be felt most strongly at low latitudes (Kraemer et al., 2017), there are incipient local studies of likely impacts on lakes and reservoirs located in subtropical regions.

The present study attempts to highlight whether potential climate projections could affect the water levels and the thermal regime in a multipurpose subtropical reservoir at the end of 2020s. Data generated by a regionalized climate model was used for hydrological and hydrodynamic simulations. The overall trends of CO_2 emissions rise have led to a change in the pattern of climate forcing data and were evaluated to understand how the reservoir water level and the thermal regime would respond in the near future. This study facilitates our current knowledge of the possible implications of climate change on subtropical lakes hydrodynamics to target possible management efforts.

2. Material and methods

2.1. Study site and input data availability

Itupararanga Reservoir is located in an urbanized region in the Alto Sorocaba basin in São Paulo State, Brazil. The reservoir's main inflow is the Sorocaba River which itself is formed by three streams: Sorocabuçu, Sorocamirim, and Una. The Sorocaba river is very important for the whole state because it is one of the main contributors to the Tietê River, a major river of São Paulo city.

The Itupararanga reservoir was built for multiple management purposes, e.g. public water supply (~2.15 $m^3\ s^{-1}$ between 2005 and 2018) that corresponds to almost 1 million of people, and power generation distributed by a private company (~11$m^3\ s^{-1}$). The hydraulic retention time of the reservoir is approx. 245 days and the average water height was 20.6 m near the dam between 2009 and 2018.

According to the Köppen-Geiger classification, the regional climate can be classified as warm and temperate with dry winter and hot summer (Cwa type; Kottek et al., 2006). The dry season occurs between April to September and the wet season is from October to March. The basin annual average rainfall was 1572 mm per year for the period of 2009–2018 (INMET, 2020). Because of the drought faced in the Southeast of Brazil in 2014, this average dropped to 1225 mm in that year. The main morphometric, hydrological, and power generation features of Itupararanga reservoir are shown in Table S1.

The catchment land-use composition is vegetation, farming (includes touristic ranches and crops) and urbanization that has increased in the last few decades (68% of the original vegetation of the watershed has been removed or replaced by farming and urbanization) (Taniwaki et al., 2013).

The trophic state of Itupararanga reservoir has shifted over the years, currently showing meso-eutrophic behavior, with a high presence of nutrients (Cunha et al., 2017; Vargas et al., 2020). The phytoplankton community has been dominated by cyanobacteria, in particular *Raphidiopsis raciborskii*, which has been proven to be toxic in the reservoir (Beghelli et al., 2016; Casali et al., 2017) and may cause impact on aquatic communities and food chains or even in the drinking water supply to population in the future.

The daily hydrological data were collected at one station located in the dam (*62510080*) since 2005. In combination with outflow data, this monitoring data were used to calculate reservoir inflows, water levels and volume.

The meteorological data were collected from Sorocaba meteorological station by National Institute of Meteorology (INMET) located 29 km from the reservoir. This station is the only source for meteorological data close to Itupararanga reservoir and it has an automatic hourly meteorological monitoring since 2006. In order to reduce bias related to those data, we performed a sensitivity analysis and calibration for model meteorological parameters.

The Environmental Company of the State of São Paulo (CETESB) has performed surface sampling every 2 months since 1998 at *SOIT02900* station, near to the dam, and since 2005 at Sorocabuçu (*SOBU02800*), Sorocamirim (*SOMI02850*) and Una (*BUNA02900*) streams. The monitoring variables include water temperature and electrical conductivity measurements. The location of Alto Sorocaba basin, its tributaries, and the monitoring stations are presented in Fig. 1.

Previous data were collected nearby the SOIT02900 station (FAPESP Projects: 2008/55636-9, 2016/09405-1) and represent measurements in the water column every 50 cm in 2009–2011, 2013–2015, and 2017–2019.

The reservoir bathymetry, which corresponds to the storage, elevation, and area relationships, were processed by a project held at the University of São Carlos's (UFSCAR-Sorocaba). This was performed by an Ecobathymetr Bathy 500-MF and the Hypack Max Software to plan, navigate, collect, and process data.

2.2. Model description

Numerical models used for ecological simulations in water bodies are subject to major developments and can be a powerful tool in studies of climate change. One-dimensional (1D) vertical process-based models are the state-of-the-art tool to simulate lake water temperature dynamics as the thermal regime in lakes has its major gradient across the vertical water column.

Those models can simulate the vertical gradients of water temperature and lake level oscillations, with low computational processing time and a high spatial as well as temporal output resolution regarding modeled state variables and fluxes, which makes them suitable to perform long term modeling analyses.

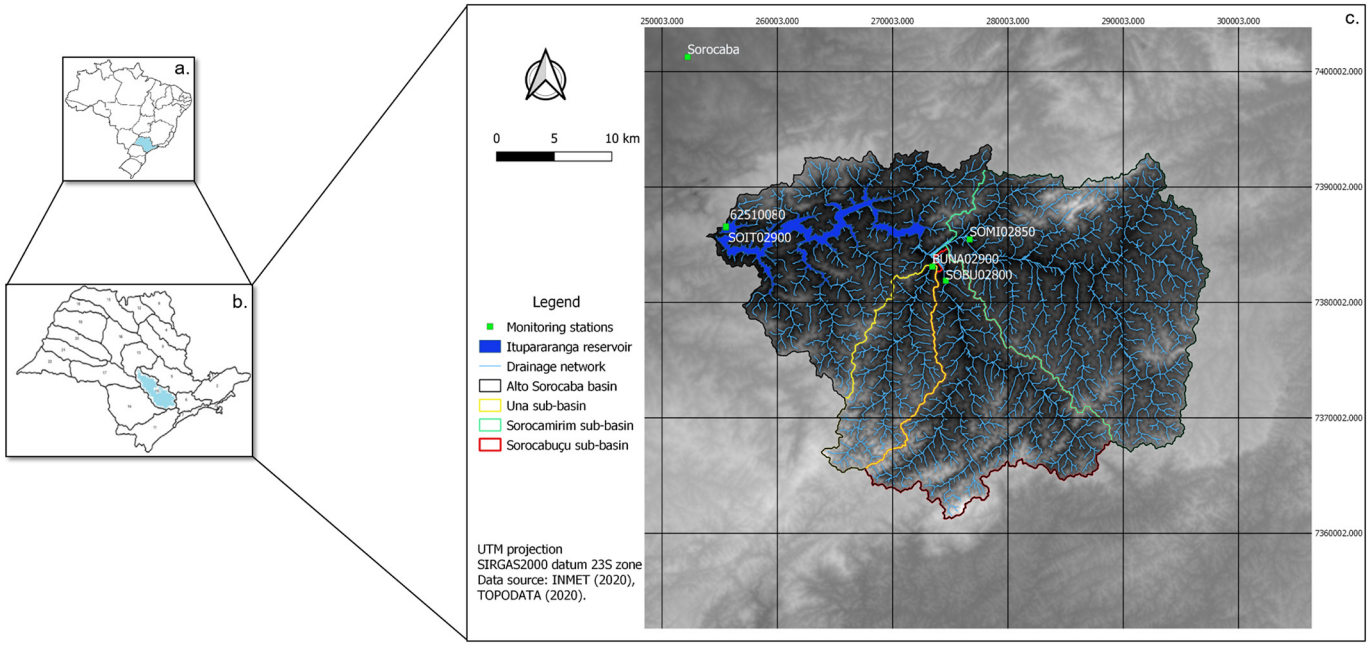

Fig. 1. Alto Sorocaba basin: a. São Paulo State location; b. Alto Sorocaba basin location; c. Itupararanga reservoir location, its tributaries and monitoring station. Data Source: INMET (2020), TOPODATA (2020)

The 1D hydrodynamic model used in the present study was the General Lake Model (GLM v.2.2.0) (Hipsey et al., 2019). The GLM simulates water balance, surface energy balance, including light penetration, sensitive and latent heat transfer, mixing regime and thermal stratification, as well as inflows, outflows, and water withdrawals. In addition, the model is open source.

The model uses the dynamic Lagrangian-layer structure (Imberger and Patterson, 1981), in which only the vertical variation is retained to resolve the vertical gradients. The contraction or expansion of layers represents lake density alterations related to mixing, stratification, and water balance. The model state variables, their processes and equations are described in the user manual (Hipsey et al., 2014).

GLM analyses were done using the statistical software R to simulate, to assess the results, and to calculate the hydrodynamic indicators through the packages glmtools (Read et al., 2016) and rLakeAnalyzer (Read et al., 2011). A geographical User Interface for GLM (glmGUI, Bueche et al., 2019) was also used for the parameter sensitivity analysis and auto-calibration.

GLM has been applied widely to understand thermal dynamics of lakes (Hipsey et al., 2017; Bruce et al., 2018; Hipsey et al., 2019) and to investigate shifts in hydrodynamics of lakes and reservoirs under climate change (Bucak et al., 2018; Soares et al., 2019; Gal et al., 2020). The model has also allowed increasing comprehension about the ecosystem processes-human actions interactions, as well as on facilitating student learning of climate change concepts (Cobourn et al., 2018; Carey and Gougis, 2016).

2.3. Data processing and modeling setup

Meteorological variables used in this study included short-wave radiation, air temperature, wind velocity, rainfall, and air relative humidity on an hourly time step (Fig. 2). Long-wave radiation was estimated from relative air humidity and air temperature (Abramowitz et al., 2012).

There is one outlet used for water withdrawal located near the bottom of the reservoir (withdrawal depth of 5.7 m). The outflow is partly used for hydroelectric power generation and partly for the local water supply. Periods of overflow occur through the reservoir spillway crest (>20.7 m elevation). The water withdrawal and the overflow were set up as separate outflows to not increase uncertainty at hydrodynamic simulation.

The incoming daily streamflow was calculated using hydraulic balance calculations by the private company that operates the dam. The streamflow conductivity was converted to salinity (Hornung, 2002). To complete missing data in the salinity time series, a mass balance calculation was performed using data from the three tributaries. Meanwhile, few electrical conductivity measurements were available. Thus, the average conductivity between the three tributaries (70.8 μS cm^{-1}) was used to estimate a mean salinity concentration that was used in the entire period (0.06 PSS). Electrical conductivity variations have not been correlated to changes in the reservoir density flow regime; instead, the freshwater reservoir's density stratification is dominantly driven by changes in water temperature (see similar inflow data and conclusions in Ryu et al., 2020).

The inflow water temperature was estimated by a weighted average of the water temperature and flows of the Sorocabuçu, Sorocamirim and Una streams. Missing data were approximated using linear interpolation on a daily time step.

We applied an automatic sensitivity analysis and calibration technique using the glmGUI v.1.0 (Bueche et al., 2019). Here, the sensitivity analysis was first conducted on water level fluctuations and secondly on changes in water temperature. Results from the sensitivity analysis guided the automatic calibration for the period from January 2009 to December 2013 (1826 days). The validation period was from January 2014 to March 2019 (1916 days).

The parameters related to minimum (h_{min}) and maximum layers thickness (h_{max}) were manually calibrated according to the reference values. The glmGUI calculates the sensitivity index (SI) for the parameters of surface dynamics, mixing parameters, and hydrological and meteorological factors The SI's considered low ($0 < SI < 0.05$) were disregarded and those considered as medium or high ($0.05 < SI < 0.2$; $0.2 < SI < 1$) were submitted to the calibration process (Lenhart et al., 2002).

Based on field observations between 2018 and 2019, indicated by four Secchi-disk measurements, the average radiation extinction coefficient (K_w) value was used as model input (0.94 m^{-1}). Hydrodynamics indicators were calculated to evaluate thermal regime at Itupararanga reservoir, e.g. annual average water level (AAWL), maximum vertical density gradient (DG), the average surface and bottom water temperature difference (SBD), retention time (RT), number of stratified days (NSD) and the Schmidt Stability Index (SSI) (Idso, 1973).

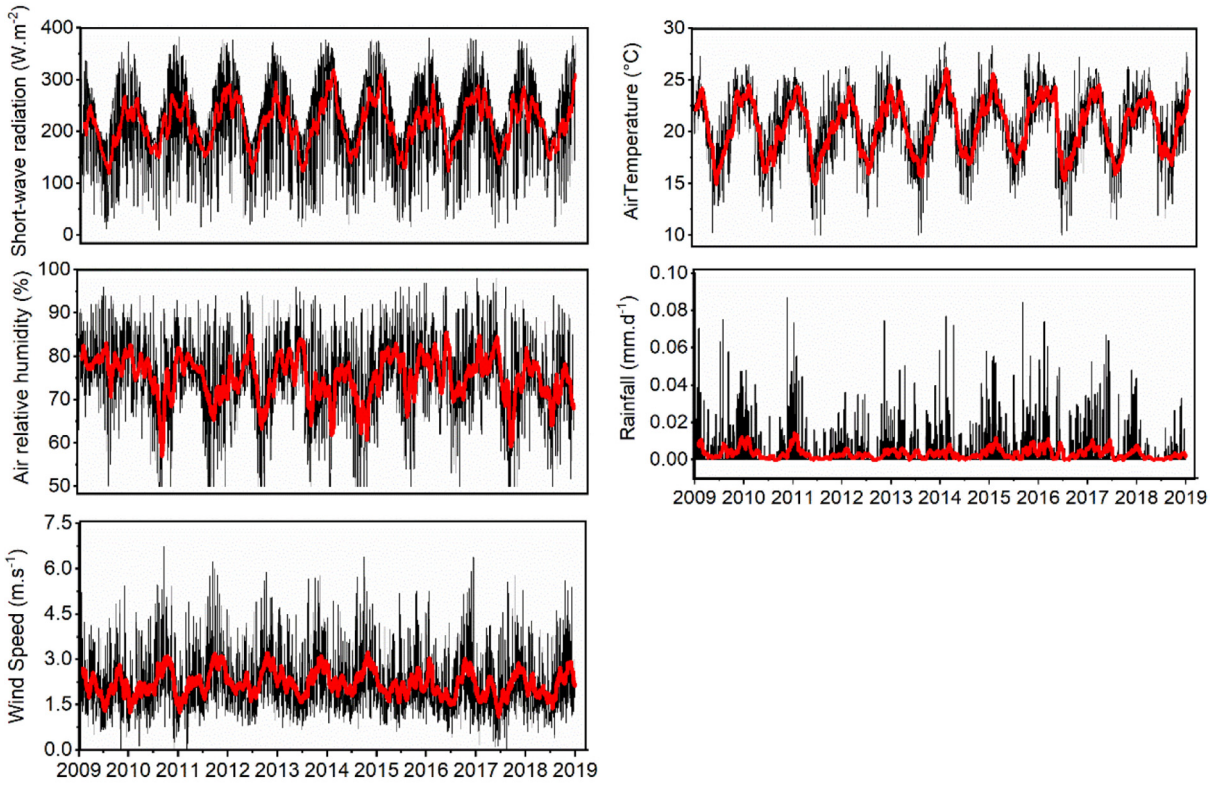

Fig. 2. Meteorological and hydrologic inputs in the simulation period. The red lines highlight simple moving average for each hydro-meteorological forcing data.

The RT, in days, was calculated from the daily flushing rate for each year. The SSI measures the energy required to mix the entire lake to a uniform temperature without the addition or subtraction of heat. As the highest SSI values were observed in the wet season, maximum SSI in the wet season (MSSw) was also calculated.

Water density was calculated by the rLakeAnalyzer package and the DGs were manually calculated between adjacent layer cells. According to Lewis (2000), for tropical lakes, a difference of 2 °C between the top and the bottom of the water column is sufficient to classify the water column as being stratified. Based on field surveys in Itupararanga reservoir, a high correlation was found between SBD and DG ($r = 0.91$). In this way, the thermal stratification was defined when the SBD > 2 °C and consequently the DG > 0.13 $kg \cdot m^3 \cdot m^{-1}$.

The model performance to simulate water level and water temperature was evaluated through Pearson's correlation coefficient (r) and the root mean squared error (RMSE):

$$RMSE = \sqrt{\frac{\sum_{i=1}^{N}(Si-Oi)2}{N}} \quad (1)$$

where: N = number of observations, S = simulated data and O = observed data for each "*i*" time step.

2.4. Hydrodynamic scenarios under climate projection

2.4.1. Data availability and processing

Data from Climate Change Projections for South America regionalized by the ETA Model (PROJETA) were used to simulate the climate change scenarios in the Itupararanga reservoir.

The global climate model (GCM) chosen was The Hadley Centre Global Environmental Model (HadGEM2-ES). The regionalization of the HadGEM2-ES projections from 2006 to 2099, carried out by the ETA model (Eta-HadGEM2-ES), had a resolution of 20 km and covers South America, Central America, and the Caribbean. The Eta-HadGEM2-ES has proved to be more sensitive to greenhouse gas (GHG) emissions and it generates improved estimations than the ETA nested in MIROC5 (Chou et al., 2014).

The scenarios were based on two GHG representative concentration pathways (RCP), which correspond to different radiative forcing scenarios of 4.5 W m^{-2} (RCP 4.5) and 8.5 W m^{-2} (RCP 8.5), respectively (Chou et al., 2014). The first one is an optimistic scenario corresponding to a CO_2 increase of about 650 ppm and the other a pessimistic scenario where CO_2 exceeds 1000 ppm in 2100.

Climatic time series by Eta-HadGEM2-ES RPC 4.5 and 8.5 included daily short-wave and long-wave radiation ($W \cdot m^2$), air temperature (°C), air humidity relative (%), rainfall (mm) and wind speed (m/s) from 2026 to 2030. A bias correction was performed to adjust historical data and correct the future projections using 1-decade data as control period (2009–2018). The long-wave radiation series was not corrected, due to the lack of observation data.

For air temperature and rainfall correction, we applied the linear and the variance scaling methods (LS/VS, Lenderink et al., 2007; Chen et al., 2011; Teutschbein and Seibert, 2012) inside of the Climate Change for Watershed Modeling tool (CMhyd, Rathjens et al., 2016). The LS method is a simple approach based on the average difference between monthly observed data and historical time series of climate models over the same period of the observed series. The VS corrects both the mean and the variance of time series. The same methods were applied to manually correct the other projected meteorological data.

2.4.2. Inflow simulation

To predict the future reservoir inflow from the climate scenarios the Soil Moisture Accounting Procedure (SMAP) was applied based on precipitation and evaporation data from the climate model.

The SMAP model uses a simple structure of reservoirs that represents the storage and water flow in the basin with continuous time series and uses the Soil Conservation Service - SCS (1964) method for the

separation of runoff. The input data are the total precipitation and evaporation heights on a daily time step, the drainage area, and the initial conditions of the basin. For calibration, the following parameters needed to be adjusted (Lopes et al., 1982): soil saturation capacity (Str), constant runoff recession (K2t), underground recharge parameter (Crec), initial abstraction (Ai), field capacity (Capc) and constant of recession of basic outflow (Kkt).

The version used in the present study was the Smap.Net version 1.0.0.0, which is freely available from the Laboratory of Decision Support Systems (LabSid-USP). The model runs and generates runoff for a limit of 1000 consecutive days.

The rainfall-runoff model was manually calibrated for 300 days, from 2010-06-23 to 2011-04-18. It was given as the initial conditions the drainage area (669 km^2), the initial soil moisture level (65 $mm \cdot mm^{-1}$), and the initial base streamflow (7 $m^3 \cdot s^{-1}$).

The goal of the calibration was to reduce the percent bias (PBIAS) for streamflow to be considered satisfactory (±25%, Moriasi et al., 1983). The calibrated model was used to estimate the reservoir future inflows based on estimated rainfall and air evaporation by Eta-HadGEM2-ES RCP 4.5 and 8.5. The air evaporation data were bias corrected using the previously cited bias correction.

The 1000 days period chosen for the simulation of the climate projections scenarios was from 2028-02-14 to 2030-11-09, which represents an exemplary time period in the near future to evaluate potential impacts of climate change on water management decisions. For the hydrological simulation, we assumed the initial base streamflow as the mean observed flow between 2009 and 2018 (13.5 $m^3 \cdot s^{-1}$).

As reservoir initial conditions for the hydrodynamic simulation, we used the monthly mean water temperatures of the last decade as daily input and the vertical salinity profiles assumed constant. Further, we used the mean lake level value and mean water temperature value for the month of January based on historical data series (2005 to 2018).

The present study did not take into account the various possibilities of water withdrawal for power generation and water supply, for simplification only a minimum daily withdrawal was considered (6.024 $m^3 \cdot s^{-1}$) based on the historical series (2005–2018). Overflows were not observed in those periods. Thermal condition indicators were calculated to quantify the climate change impact on the reservoir thermal regime.

3. Results

3.1. Model performance

The Sensitivity analysis for water level and water temperature presented variations between the parameters and the evaluated multiplicative factors (Fig. 3). The water level had high sensitivity to the inflows and outflows factors (SI = 0.54 and 0.69, respectively) and medium sensitivity to the rain factor (SI = 0.15).

Regarding water temperature, the sensitivity analysis highlighted the model's medium sensitivity to the wind factor (SI = 0.18) and high sensitivity (SI = 0.21) to the latent heat transfer coefficient (c_e). Sensitive parameters were automatically calibrated, and the minimum and maximum layer thickness were manually adjusted (Table S2).

The calibrated and validated water level and water temperature of the Itupararanga reservoir showed good model fit criteria (Fig. 4, Table 1). For calibration, Pearson correlation results showed higher values at 5 m, 10 m, and 15 m than in the top surface layer. On the other hand, for the validation period, the highest Pearson correlation was found at 5 m, followed by top surface layer, and the simulated bottom waters were warmer than the observations.

The simulated thermocline depths were compared with field observations to evaluate the model performance to observed mixing dynamics in the Itupararanga reservoir (Fig. S1). The thermocline depths were usually measured between 6.5 and 14 m and the simulations achieved a range between 6 and 16.5 m, highlighting a thermocline deepening bias (PBIAS = −17).

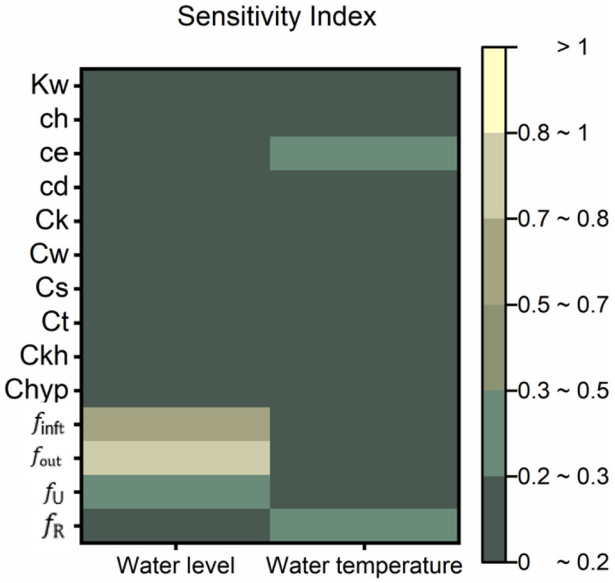

Fig. 3. Sensitivity index for water level and water temperature. Kw = light extinction coefficient; Non-neutral bulk-transfer coefficients: ch = sensible heat transfer, ce = latent heat transfer, cd = momentum; Mixing parameters: C_K = efficiency of convective overturn, C_W = efficiency of wind stirring, C_S = efficiency of shear production, C_t = efficiency of unsteady turbulence, C_{kh} = efficiency of Kelvin–Helmholtz billowing, C_{hyp} = efficiency of hypolimnetic turbulence; Multiplicative factors: f_{inft} = inflow, f_{out} = outflow, f_U = rain, f_R = wind.

3.2. Hydrodynamics indicators

The hydrodynamics indicators of Itupararanga reservoir in the simulation period are given in Table S3.

A lower NSD was identified in 2014 (72 days) compared to the entire simulated period. On the other hand, after the rising lake level in the year 2015, the SBD achieved 1.79 °C and the NSD increased (136 days). Besides, the highest MSSw was accounted at 2018-12-21 (135.9 $J \cdot m^{-2}$), followed by 116 $J \cdot m^{-2}$ at 2015-01-12 (shortly after the drought period).

In the summer of 2014, the monthly mean precipitation was 140.7 mm (INMET, 2020). In January 2014, the measured rainfall was 85 mm, the lowest accumulated between 2008 and 2018. There was an increase in

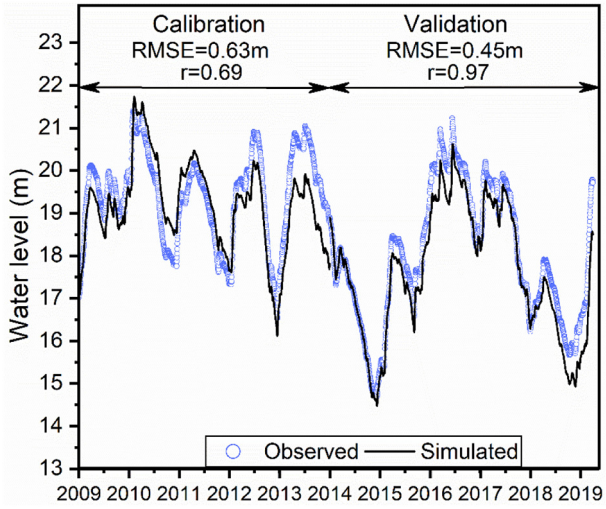

Fig. 4. Observed and simulated water level.

Table 1
Model performance metrics in four specific depths and water column over the simulation period.

Depths (m)	Calibration					Validation				
	0	5	10	15	Water column	0	5	10	15	Water column
RMSE (°C)	1.74	0.67	2.41	1.36	1.30	1.73	0.69	1.85	2.0	1.34
r	0.84	0.98	0.91	0.97	0.83	0.90	0.97	0.81	0.78	0.81

rainfall in the wet season of 2015 and this led to changes in the reservoir's thermal regime. Between 2014 and 2015 the daily reservoir volume was below the mean volume observed from 2008 to 2018 that corresponded to $204 \cdot 10^6$ m^3 (INMET, 2020). The daily average minimum volume was $115 \cdot 10^6$ m^3 in December 2014.

3.3. Bias-corrected climate series and simulation of inflows

We corrected the simulated historical climate data from the global climate model HadGEM2-ES regionalized by the ETA model under two downscaling scenarios (RCP 4.5 and 8.5) using the linear and variance scaling approach. After the observed and simulated historical climate data had been compared and the identified biases, parameterized bias correction based on the mean and the variance of times series was used to correct historical and future climate data. (Table S4).

The forecasted climate data showed significant differences regarding the baseline period (see Fig. S2). A slight future increase in shortwave radiation and wind speed are expected for the two GHG increase scenarios.

The projections indicate an average air temperature increase of 2.5 °C (RCP 4.5) and 3.3 °C (RCP 8.5) relative to the baseline for the end of this decade and beginning of the next one. On the other hand, the average rainfall and relative humidity showed a downward trend.

The calibrated parameters of the hydrological model are shown in Table S5. Although the observed inflow peak (January 2011) was overestimated by 37% compared to the simulation in the calibration (see Fig. S3), the SMAP presented satisfactory performance (PBIAS = 18%; $\pm 15 \leq$ PBIAS $< \pm 25$, Moriasi et al., 1983) to predict minimum and mean inflows.

After the calibration, the SMAP model was able to simulate representative future inflows from 2028-02-14 to 2030-11-09 (Fig. S4). In the pessimistic scenario, the average daily inflows were well below (2.6 m$^3 \cdot$s^{-1}) the historical baseline (13.5 m$^3 \cdot$s^{-1}), despite a simulated peak in November 2028 (52.2 m$^3 \cdot$s^{-1}) that exceed the baseline flow. On the other hand, for the optimistic scenario, the simulated inflows showed a similar behavior of decreasing discharges during the drought period observed in 2014 and during the wet period in 2018 (Fig. S4).

3.4. Climate scenarios for the Itupararanga reservoir

The annual average water level showed a declining trend in the optimistic scenario (Fig. 5; 20.5 m, 18.4 m and 15.4 m for the years of 2028, 2029 and 2030, respectively). In 2014, the Itupararanga water level has reached a historical minimum of 16.7 m. On the other hand, in the pessimistic scenario, the water level declined with a higher rate than the optimistic scenario (20.7 m in 2028, 16.3 m in 2029, reaching and remaining at dead storage in the whole year of 2030).

The warming of the top layer was evident in both scenarios; the annual average water temperature reached 22.6 °C in the pessimistic scenario (Table 2). The SBD was higher in the RCP 4.5 scenario than in the RCP 8.5 one. This higher difference between surface and bottom temperatures results in an increased water column stability.

The minimum annual depth of the thermocline was at 6 m from the surface for the optimistic scenario and at 4 m for the pessimistic one. The maximum depth was at 18 m for both scenarios. On the other hand, in the period of reservoir dead storage, the thermocline remained more shallow (10 m < RCP4.5 < 11 m; 6 m < RCP8.5 < 10 m).

The SSI values increased in both scenarios (MSSW > 150 J$\cdot$m^{-2}) when compared to the baseline (Table S3 and Fig. S5). The thermal stability of the Itupararanga reservoir will increase (Fig. 6) and stratification periods would start earlier (before spring).

4. Discussion

4.1. Evaluation of model performance and hydrodynamics features of Itupararanga reservoir

The water level simulation results suggest a good fit with the observations (RMSE < 0.63 m, $r > 0.8$). Previous studies using 1D models

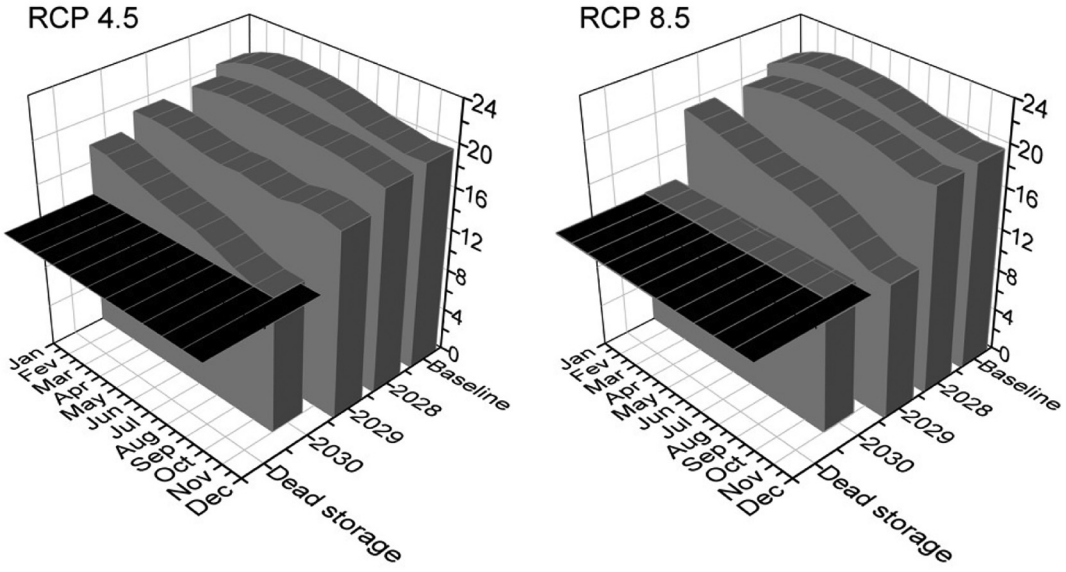

Fig. 5. Water levels under RCP 4.5 and 8.5 scenarios in 2028, 2029 and 2030. Baseline: monthly average depth from 2009 to 2018.

Table 2
Comparison between thermal conditions indicators for calibration and validation period and future optimistic (RCP 4.5) and pessimistic (RCP 8.5) scenarios.

Thermal conditions indicators	2009–2013	2014–2018	2028–2030	
			RCP 4.5	RCP 8.5
Average surface temperature (°C)	21.0	21.6	22.2	22.6
Average bottom temperature (°C)	20.1	20.8	19.6	20.4
SBD (°C)	0.9	0.8	2.6	2.2
Percentage of stratified days (%)	24	30	53	36

have shown similar agreements (0.2 m < RMSE < 0.74 m; Fadel et al., 2017; Melo et al., 2019; Bueche et al., 2019). Furthermore, the model showed a good capability to predict short-term water fluctuations, especially between 2014 and 2015, when the reservoir volume decreased to ~29% of its normal capacity (Fig. 4).

The achieved model fit for temperature profile simulation can be evaluated as very satisfactory (RMSE < 1.4 °C, Table 1). The literature reports to the whole water column an acceptable range of RMSE between 0.9 °C and 1.5 °C (Bueche and Vetter, 2014; Fenocchi et al., 2017; Prats et al., 2018). Recently, Farrell et al. (2020) showed that the uncertainties associated with water temperature simulations from manual and buoy data were similar and have a low influence on projections. Additionally, the study highlighted that the thermal simulations were better in the epilimnion than the hypolimnion. In the present study, when water temperatures at certain specific depths (surface, 5, 10, and 15 m) were evaluated, the error adjustments increased (RMSE ~ 1.7 °C) suggesting a trend to overestimate water temperature in the bottom and underestimate water temperatures in the surface layers. This highlights the influence of the meteorological boundary conditions on the model performance.

In the same way, a warm bias for the hypolimnetic temperature simulations had previously been reported (Bruce et al., 2018), as well as a bias in the prediction of the thermocline depth (Bruce et al., 2018; Bueche et al., 2017). In the present study, the simulation of thermocline depth achieved a satisfactory agreement compared to observations (Fig. S1).

Another important finding was that in the drought period (2014–2015), the outflow was reduced, which eventually increased the hypothetical RT (453 days) to maintain a secure power generation and drinking water supply (see Table S3). In the same period, the water level dropped, and it influenced the thermal conditions of the Itupararanga reservoir (NSD = 72 days and MSSw = 75.9 $J \cdot m^{-2}$). Similar behavior was identified in the Serra Azul reservoir, MG-Brazil, between 2014 and 2015, with a decrease of the number of stratified days due to a decrease in water level (Soares et al., 2019).

Prior studies have identified that lakes and reservoirs respond rapidly to climate change (Adrian et al., 2009) and the shifts on rainfall regime favors intensification of lake levels fluctuations (Reichstein et al., 2013). A recent decrease in the annual average rainfall was recorded in 2018 (INMET, 2020) leading to a decline of water level and a raise of MSSw (135.9 $J \cdot m^{-2}$). This may be a consequence of increased air temperature and consequentially the heating of the surface layer (Darko et al., 2019).

4.2. Climatic data bias correction and hydrological calibration

Technical improvements of the output data from RCMs and their application to study the hydrological impacts of climate change has developed in the last decade (Chen et al., 2011; Chen et al., 2013). However, data bias corrections are still used to reduce the uncertainties of the simulations.

Climate projections were corrected using current data and bias correction techniques. The linear and variance scaling techniques, based on simple statistical methods (mean and variance), showed good agreement (Table S4) within the range of results available in the literature (Li et al., 2019; Eccles et al., 2019; Teutschbein and Seibert, 2012).

The calibration of a simple hydrological model was performed to simulate future inflows to the Itupararanga reservoir. Despite that the observed maximum discharge (54.4 $m^3 \cdot s^{-1}$) has been overestimated by 27% in the model (Fig. 5), generally the SMAP model showed a good accuracy ($r = 0.67$) to replicate the inflow dynamics. Additional monitoring stations for discharges would need required to improve the simulation results.

Similar results were achieved by Cavalcante et al. (2020) calibrating measured flash flood from eight rain gauges in the mountainous region of Rio de Janeiro, Brazil. Despite the calibration limitations, a previous study reported that the SMAP model was capable to predict future inflows for a hydroelectric plant based on data from an RCM, especially after the rainfall bias correction (da Silva et al., 2019).

4.3. Water supply implications for the Itupararanga reservoir at the end of this decade

Two scenarios (based on optimistic (RCP 4.5) and pessimistic (RCP 8.5) climate projections concerning GHG) were simulated using the hydrodynamic model. To run these scenarios the bias-corrected climate

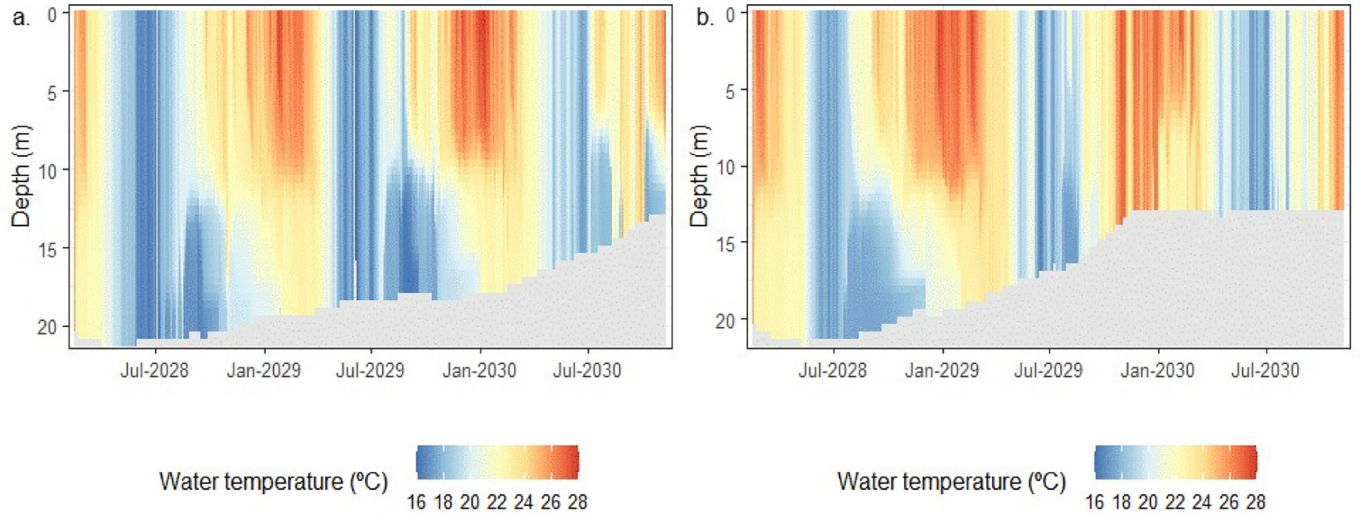

Fig. 6. Simulated water temperature: a. RCP 4.5 scenario b. RCP 8.5 scenario.

projections and the simulated inflows were set as boundary conditions to GLM.

The decrease in the air evaporation rates and the average daily rainfall in the analyzed period led to a decrease in the future inflows, assuming historical minimum outflow conditions in the reservoir (Figs. S2 and S4). Bucak et al. (2018) also reported a trend of decreasing future total inflows under RCP 4.5 and 8.5 conditions in 2030 and 2060 based on land-use changes for a large lake in Turkey.

Our simulations suggest that the local water supply from the reservoir works will be scarcely limited by October 2030 in the optimistic scenario due to future lower daily rainfall in the watershed and the, although low, withdrawal within the reservoir itself. On the other hand, in the pessimistic scenario, the reservoir may not be able to provide enough water already beginning in December 2029 as it had reached dead storage (Fig. 5).

The generalizability of the achieved results is subject to certain limitations. For instance, we are limited in predicting future outflow changes as well as shifts in the land-use of the catchment, which could cause feedback reactions on the reservoir's volume and thermal dynamics. In another study, under current land-use conditions and the HadGEM model under RCP 4.5 data, predictions until 2030 of the Lake Beyşehir had indicated a drop in the water level and for the RCP 8.5 scenario a slight increase (Bucak et al., 2018).

The simulated scenarios highlight that the water management needs to avoid future water losses in the Itupararanga reservoir water supply. During the drought period (2014 to 2015), management used the reservoir dead storage, however it was not possible to supply drinking water to the almost 1 million inhabitants and there was a need for water rationing in some cities. Due to a decrease in the volume of the Itupararanga reservoir in 2018, the population was advised to save water to avoid new rationing.

Despite the fact that a lake's water storage can be influenced by climate change, there exist a large regional variability that interacts with it (Woolway et al., 2020; Shatwell et al., 2019). For example, strong seasonal variations regarding rainfall regime (dry and wet periods in the region), as well as lake-specific factors, such as morphometry. Further, reservoirs operation can play an important role to maintain appropriate water levels.

4.4. Consequences in the reservoir thermal regime based on climate projections

In both simulated scenarios the average surface water temperature increased compared to model calibration and validation periods (RCP 4.5: +1.1 °C (2009–2013), RCP 8.5: +1.6 °C (2009–2013), RCP 4.5: +0.6 °C (2014–2018), RCP8.5: +1.1 °C (2014–2018)). The literature has reported that lake surface temperatures have raised worldwide similarly to air temperature trends (O'Reilly et al., 2015; Woolway et al., 2019; Farrell et al., 2020).

The heating trend along the water column has also been reported (Pilla et al., 2018; Shatwell et al., 2019; Mi et al., 2020). In Itupararanga reservoir, the SBD measured was −1 °C between 2008 and 2018 and for the optimistic and pessimistic scenarios, it will increase by +2 °C for the period between 2028 and 2030 (Table 2), which would increase thermal stratification. Due to climate change, many lakes across the world may mix less frequently and alter their thermal regimes (Woolway and Merchant, 2019).

The optimistic scenario projects future stratification from October to mid-July/August (53% of stratified days in the entire simulated period, see Fig. 6a). This occurs in conjunction with rainfall regime changes (an increase of 38% between July and September compared to the historical time series).

On the other hand, the percentage of stratified days was lower for the pessimistic scenario (36%) compared to the RCP 4.5, prolonging the amount of mixing days (Fig. 6b). This downward trend in stratified days may be related to the decrease in water level (shown in Section 4.1) that favors the heating of the total water column and vertical mixing of water masses (Magee and Wu, 2017).

The simulated thermocline depth has also shifted in both scenarios. Higher GHC emission scenarios predicted thermocline deepening. Similar behaviors have been forecasted for Lake Maggiore and Lake Tegel, with an intensification of the summer stratification period and an increase of thermocline depth (Fenocchi et al., 2018; Ladwig et al., 2018).

The stratified days and the thermocline depth are projected to increase in Itupararanga reservoir, as well as the water column stability (Fig. S5). Our model also predicted that the lakes thermal stability (SSI) is projected to increase in the future, resulting in strengthened stratification and reduced vertical exchange between surface and bottom layers (Darko et al., 2019; Niedrist et al., 2018).

The literature has highlighted cyanobacteria predominance in the last 20 years in the Itupararanga reservoir (Beghelli et al., 2016; Cunha and Calijuri, 2011). Such dominance was driven by high water temperatures, especially in the summer, and high concentrations of ammonium and nitrate available in the reservoir (Cunha et al., 2017). Casali et al. (2017) also showed evidence of correlation between high concentrations of dissolved nutrients and higher densities of *Raphidiopsis raciborskii* (Cyanobacteria), as well as concentrations of saxitoxins in the water.

A recent study highlighted that the RCP 8.5 projections are closer to historical projections and have been predicted as the best combination for 2030 and 2050 based on current GHG emission policies (Schwalm et al., 2020). Further investigation needed to be done to better assess the impacts on reservoir water quality by water level fluctuations. Periods of drought have been related to the increase in trophic state and consequent blooming of cyanobacteria (Tundisi et al., 2015; Brasil et al., 2016; Mantzouki et al., 2018).

Under surface water heating, thermal stability intensification and a lengthening of the stratification duration, water quality could potentially deteriorate (Gray et al., 2019; Huisman et al., 2018). A potential trophic level increase may prevent some reservoir uses, such as navigation and fishing, and generate high costs to improve drinking water treatment. Therefore, water management needs to assess likely future impacts and decision-making needs.

5. Conclusion

The current study investigates the impacts of future scenarios on the hydrodynamics of a Brazilian multipurpose reservoir. Meteorological projections based on a one low CO_2 emissions (RCP 4.5) scenario and a high-emission pathway with no climate policy (RCP 8.5) scenario were incorporated in a simple hydrologic model and a process-based hydrodynamic model.

In two scenarios of GHG emissions and minimum water withdrawal by the reservoir management, the water level was projected to decrease and fall to the reservoir dead storage. Consequently, there could be a future lack of water supply and decrease of power generation for a region with a population of almost 1 million of people. The intensity of CO_2 emissions has been shown to have a strong correlation with the meteorological variables. The daily rainfall projections were lower for 2028–2030 in comparison to the long-term historical data, showing a negative correlation with the GHG emissions raise. In the RCP 8.5 scenario, the dead volume would be reached in 2029, while in the optimistic scenario, the reservoir would become unusable 10 months later.

On the other hand, air temperature projections had a positive correlation with the CO_2 emissions scenarios. Consequently, surface water temperatures tend to increase in both simulated scenarios. Furthermore, longer periods of thermal stratification and a projected rise of water column stability are expected and may generate harmful consequences for aquatic biota and water quality.

Further research should focus on determining climate effects on the aquatic ecosystem, especially regarding harmful cyanobacteria that can cause many issues. The insights gained from this study may be of

assistance to support management measures to ensure the maintenance of reservoir uses and water quality considering future climate projections.

Code and data availability

The GLM source code and several test cases are available, accessible at https://aquatic.science.uwa.edu.au/research/models/GLM/latest_release and the SMAP model is available online at http://pha.poli.usp.br/default.aspx?id=76&link_uc=disciplina. The climate projections data regionalized by the ETA model are available online at https://projeta.cptec.inpe.br/.

CRediT authorship contribution statement

Carolina Cerqueira Barbosa: Writing – original draft, Writing – review & editing, Conceptualization, Methodology, Software, Visualization. **Maria do Carmo Calijuri:** Supervision, Resources, Writing – review & editing, Writing – original draft. **André Cordeiro Alves dos Santos:** Writing – review & editing, Data curation. **Robert Ladwig:** Writing – review & editing, Visualization. **Lais Ferrer Amorim de Oliveira:** Writing – review & editing, Methodology. **Ana Carolina Sarmento Buarque:** Writing – review & editing, Visualization.

Declaration of competing interest

The authors declare that they have no known competing financial interests or personal relationships that could have appeared to influence the work reported in this paper.

Acknowledgements

The authors are grateful to the INMET, CETESB, UFSCAR-Sorocaba for provision of the available data. The authors express their sincere thanks to Dr. Davi G.F. Cunha, Dr. Simone P. Casali, Dr. Munique A. B. Moraes and Msc. Gabriela A. Marafão for providing the water temperature profiles for the Itupararanga reservoir. The authors also acknowledge the Coordenação de Aperfeiçoamento de Pessoal de Nível Superior (CAPES) for the financial support.

Appendix A. Supplementary data

Supplementary data to this article can be found online at https://doi.org/10.1016/j.scitotenv.2020.144741.

References

Abramowitz, G., Pouyanné, L., Ajami, H., 2012. On the information content of surface meteorology for downward atmospheric long-wave radiation synthesis. Geophys. Res. Lett. 39, L04808. https://doi.org/10.1029/2011GL050726.

Adrian, R., O'Reilly, C.M., Zagarese, H., Baines, S.B., Hessen, D.O., Keller, W., Livingstone, D.M., Sommaruga, R., Straile, D., Van Donk, E., Weyhenmeyer, G.A., Winder, M., 2009. Lakes as sentinels of climate change. Limnol. Oceanogr. 54, 2283–2297. https://doi.org/10.4319/lo.2009.54.6_part_2.2283.

Beghelli, F.G., Frascareli, D., Pompêo, M.L.M., Moschini-Carlos, V., 2016. Trophic state evolution over 15 years in a tropical reservoir with low nitrogen concentrations and cyanobacteria predominance. Water Air Soil Pollut. 227. https://doi.org/10.1007/s11270-016-2795-1.

Brasil, J., Attayde, J.L., Vasconcelos, F.R., Dantas, D.D.F., Huszar, V.L.M., 2016. Drought-induced water-level reduction favors cyanobacteria blooms in tropical shallow lakes. Hydrobiologia 770, 145–164. https://doi.org/10.1007/s10750-015-2578-5.

Bruce, L.C., Frassl, M.A., Arhonditsis, G.B., Gal, G., Hamilton, D.P., Hanson, P.C., Hetherington, A.L., Melack, J.M., Read, J.S., Rinke, K., Rigosi, A., Trolle, D., Winslow, L., Adrian, R., Ayala, A.I., Bocaniov, S.A., Boehrer, B., Boon, C., Brookes, J.D., Bueche, T., Busch, B.D., Copetti, D., Cortés, A., de Eyto, E., Elliott, J.A., Gallina, N., Gilboa, Y., Guyennon, N., Huang, L., Kerimoglu, O., Lenters, J.D., MacIntyre, S., Makler-Pick, V., McBride, C.G., Moreira, S., Özkundakci, D., Pilotti, M., Rueda, F.J., Rusak, J.A., Samal, N.R., Schmid, M., Shatwell, T., Snorthheim, C., Soulignac, F., Valerio, G., van der Linden, L., Vetter, M., Vinçon-Leite, B., Wang, J., Weber, M., Wickramaratne, C., Woolway, R.I., Yao, H., Hipsey, M.R., 2018. A multi-lake comparative analysis of the General Lake Model (GLM): stress-testing across a global observatory network. Environ. Model. Softw. 102, 274–291. https://doi.org/10.1016/j.envsoft.2017.11.016.

Bucak, T., Trolle, D., Tavşanoğlu, Ü.N., Çakıroğlu, A.İ., Özen, A., Jeppesen, E., Beklioğlu, M., 2018. Modeling the effects of climatic and land use changes on phytoplankton and water quality of the largest Turkish freshwater lake: Lake Beyşehir. Sci. Total Environ. 621, 802–816. https://doi.org/10.1016/j.scitotenv.2017.11.258.

Bueche, T., Vetter, M., 2014. Simulating water temperatures and stratification of a prealpine lake with a hydrodynamic model: calibration and sensitivity analysis of climatic input parameters. Hydrol. Process. 28, 1450–1464. https://doi.org/10.1002/hyp.9687.

Bueche, T., Hamilton, D.P., Vetter, M., 2017. Using the General Lake Model (GLM) to simulate water temperatures and ice cover of a medium-sized lake: a case study of Lake Ammersee, Germany. Environ. Earth Sci. 76, 1–14. https://doi.org/10.1007/s12665-017-6790-7.

Bueche, T., Wenk, M., Poschlod, B., Giadrossich, F., Pirastru, M., Vetter, M., 2019. glmGUI v1.0: an R-based geographical user interface and toolbox for GLM (General Lake Model) simulations. Geosci. Model Dev. Discuss. https://doi.org/10.5194/gmd-2018-314.

Carey, C.C., Gougis, R.D., 2016. Simulation modeling of lakes in undergraduate and graduate classrooms increases comprehension of climate change concepts and experience with computational tools. J. Sci. Educ. Technol. 26, 1–11. https://doi.org/10.1007/s10956-016-9644-2.

Casali, S.P., Santos, A.C.A., Bortoletto De Falco, P., Calijuri, M. do C., 2017. Influence of environmental variables on saxitoxin yields by *Cylindrospermopsis raciborskii* in a mesotrophic subtropical reservoir. J. Water Health, 509–518 https://doi.org/10.2166/wh.2017.266.

Cavalcante, M.R.G., Barcellos, P. da C.L., Cataldi, M., 2020. Flash flood in the mountainous region of Rio de Janeiro state (Brazil) in 2011: part I—calibration watershed through hydrological SMAP model. Nat. Hazards 102, 1117–1134. https://doi.org/10.1007/s11069-020-03948-3.

Chen, J., Brissette, F.P., Leconte, R., 2011. Uncertainty of downscaling method in quantifying the impact of climate change on hydrology. J. Hydrol. 401, 190–202. https://doi.org/10.1016/j.jhydrol.2011.02.020.

Chen, J., Brissette, F.P., Chaumont, D., Braun, M., 2013. Performance and uncertainty evaluation of empirical downscaling methods in quantifying the climate change impacts on hydrology over two North American river basins. J. Hydrol. 479, 200–214. https://doi.org/10.1016/j.jhydrol.2012.11.062.

Chou, S.C., Lyra, A., Mourão, C., Dereczynski, C., Pilotto, I., Gomes, J., Bustamante, J., Tavares, P., Silva, A., Rodrigues, D., Campos, D., Chagas, D., Sueiro, G., Siqueira, G., Marengo, J., 2014. Assessment of Climate Change over South Downscaling Scenarios. pp. 512–527.

Cobourn, K.M., Carey, C.C., Boyle, K.J., Duffy, C., Dugan, H.A., Farrell, K.J., Fitchett, L., Hanson, P.C., Hart, J.A., Henson, V.R., Hetherington, A.L., Kemanian, A.R., Rudstam, L.G., Shu, L., Soranno, P.A., Sorice, M.G., Stachelek, J., Ward, N.K., Weathers, K.C., Weng, W., Zhang, Y., 2018. From concept to practice to policy: modeling coupled natural and human systems in lake catchments. Ecosphere 9, 1–15. https://doi.org/10.1002/ecs2.2209.

Cunha, D.G.F., Calijuri, M. do C., 2011. Lake and reservoir management limiting factors for phytoplankton growth in subtropical reservoirs: the effect of light and nutrient availability in different longitudinal compartments. Lake Reserv. Manag. 27 (2), 162–172. https://doi.org/10.1080/07438141.2011.574974org/10.1080/07438141.2011.574974.

Cunha, D.G.F., Lima, V.F.M., Néri, A.M., Marafão, G.A., Miwa, A.C.P., Calijuri, M. do C., Bendassoli, J.A., Tromboni, F., Maranger, R., 2017. Uptake rates of ammonium and nitrate by phytoplankton communities in two eutrophic tropical reservoirs. Int. Rev. Hydrobiol. 102, 125–134. https://doi.org/10.1002/iroh.201701900.

Darko, D., Trolle, D., Asmah, R., Bolding, K., Adjei, K.A., Odai, S.N., 2019. Modeling the impacts of climate change on the thermal and oxygen dynamics of Lake Volta. J. Great Lakes Res. 45, 73–86. https://doi.org/10.1016/j.jglr.2018.11.010.

Eccles, R., Zhang, H., Hamilton, D., 2019. A review of the effects of climate change on riverine flooding in subtropical and tropical regions. J. Water Clim. Chang. https://doi.org/10.2166/wcc.2019.175.

Fadel, A., Lemaire, B.J., Vinçon-Leite, B., Atoui, A., Slim, K., Tassin, B., 2017. On the successful use of a simplified model to simulate the succession of toxic cyanobacteria in a hypereutrophic reservoir with a highly fluctuating water level. Environ. Sci. Pollut. Res. 24, 20934–20948. https://doi.org/10.1007/s11356-017-9723-9.

Farrell, K.J., Ward, N.K., Krinos, A.I., Hanson, P.C., Daneshmand, V., Figueiredo, R.J., Carey, C.C., 2020. Ecosystem-scale nutrient cycling responses to increasing air temperatures vary with lake trophic state. Ecol. Model. 430, 109134. https://doi.org/10.1016/j.ecolmodel.2020.109134.

Fenocchi, A., Rogora, M., Sibilla, S., Dresti, C., 2017. Relevance of inflows on the thermodynamic structure and on the modeling of a deep subalpine lake (Lake Maggiore, Northern Italy/Southern Switzerland). Limnologica 63, 42–56. https://doi.org/10.1016/J.LIMNO.2017.01.006.

Fenocchi, A., Rogora, M., Sibilla, S., Ciampittiello, M., Dresti, C., 2018. Forecasting the evolution in the mixing regime of a deep subalpine lake under climate change scenarios through numerical modelling (Lake Maggiore, Northern Italy/Southern Switzerland). Clim. Dyn., 1–16 https://doi.org/10.1007/s00382-018-4094-6.

Gal, G., Yael, G., Noam, S., Moshe, E., Schlabing, D., 2020. Ensemble modeling of the impact of climate warming and increased frequency of extreme climatic events on the thermal characteristics of a sub-tropical lake. Water 12 (1982), 1–20. https://doi.org/10.3390/w12071982.

Gray, E., Elliott, J.A., Mackay, E.B., Folkard, A.M., Keenan, P.O., Jones, I.D., 2019. Modelling lake cyanobacterial blooms: disentangling the climate - driven impacts of changing mixed depth and water temperature. Freshw. Biol. 23, 1–15. https://doi.org/10.1111/fwb.13402.

Griggs, D., Stafford-Smith, M., Gaffney, O., Rockstrom, J., Ohman, M.C., Shyamsundar, P., Steffen, W., Glaser, G., Kanie, N., Noble, I., 2013. Sustainable development goals for people and planet. Nature 495, 305–307.

Hipsey, M.R., Bruce, L.C., Hamilton, D.P., 2014. GLM - General Lake Model: Model Overview and User Information. The University of Western Australia, Perth, Australia.

Hipsey, Matthew R., Bruce, L.C., Boon, C., Busch, B., Carey, C.C., Hamilton, D.P., Hanson, P.C., Moo, J., Read, J.S., de Sousa, E., Weber, M., Winslow, L.A., 2017. A General Lake Model (GLM) for simulation within the Global Lake Ecological Observatory Network (GLEON). Geosci. Model Dev. https://doi.org/10.5194/gmd-2017-257.

Hipsey, M.R., Bruce, L.C., Boon, C., Busch, B., Carey, C.C., Hamilton, D.P., Hanson, P.C., Read, J.S., de Sousa, E., Weber, M., Winslow, L.A., 2019. A General Lake Model (GLM 3.0) for linking with high-frequency sensor data from the Global Lake Ecological Observatory Network (GLEON). Geosci. Model Dev. 12, 473–523. https://doi.org/10.5194/gmd-12-473-2019.

Hornung, R., 2002. Numerical Modelling of Stratification in Lake Constance With the 1-D Hydrodynamic Model DYRESM (Thesis).

Huisman, J., Codd, G.A., Paerl, H.W., Ibelings, B.W., H Verspagen, J.M., Visser, P.M., 2018. Cyanobacterial blooms. Nat. Rev. Microbiol. 16, 471–483. https://doi.org/10.1038/s41579-018-0040-1.

Idso, S.B., 1973. On the concept of lake stability. Limnol. Oceanogr. 18 (4), 681–683. https://doi.org/10.4319/lo.1973.18.4.0681.

Imberger, J., Patterson, J.C., 1981. A dynamic reservoir simulation model - DYRESM: 5. Transport Models/Inland & Coastal Waters. Elsevier, pp. 310–361 https://doi.org/10.1016/B978-0-12-258152-6.50014-2.

INMET, 2020. Automatic monitoring stations. https://mapas.inmet.gov.br/. (Accessed 18 January 2020).

IPCC, 2014. In: Core Writing Team, Pachauri, R.K., Meyer, L.A. (Eds.), Climate Change 2014: Synthesis Report. Contribution of Working Groups I, II and III to the Fifth Assessment Report of the Intergovernmental Panel on Climate Change. IPCC, Geneva, Switzerland (151 pp.).

Jeppesen, E., Brucet, S., Naselli-Flores, L., Papastergiadou, E., Stefanidis, K., Nõges, T., Nõges, P., Attayde, J.L., Zohary, T., Coppens, J., Bucak, T., Menezes, R.F., Freitas, F.R.S., Kernan, M., Søndergaard, M., Beklioğlu, M., 2015. Ecological impacts of global warming and water abstraction on lakes and reservoirs due to changes in water level and related changes in salinity. Hydrobiologia. https://doi.org/10.1007/s10750-014-2169-x.

Jeppesen, E., Søndergaard, M., Liu, Z., Jeppesen, E., Søndergaard, M., Liu, Z., 2017. Lake restoration and management in a climate change perspective: an introduction. Water 9, 122. https://doi.org/10.3390/w9020122.

Kosten, S., Huszar, V.L.M., Bécares, E., Costa, L.S., Donk, E., Hansson, L.-A., Jeppesen, E., Kruk, C., Lacerot, G., Mazzeo, N., Meester, L., Moss, B., Lürling, M., Nõges, T., Romo, S., Scheffer, M., 2012. Warmer climates boost cyanobacterial dominance in shallow lakes. Glob. Chang. Biol. 18, 118–126. https://doi.org/10.1111/j.1365-2486.2011.02488.x.

Kottek, M., Grieser, J., Beck, C., Rudolf, B., Rubel, F., 2006. World map of the Köppen-Geiger climate classification updated. Meteorol. Zeitschrift 15, 259–263. https://doi.org/10.1127/0941-2948/2006/0130.

Kraemer, B.M., Chandra, S., Dell, A.I., Dix, M., Kuusisto, E., Livingstone, D.M., Schladow, S.G., Silow, E., Sitoki, L.M., Tamatamah, R., McIntyre, P.B., 2017. Global patterns in lake ecosystem responses to warming based on the temperature dependence of metabolism. Glob. Chang. Biol. 23. https://doi.org/10.1111/gcb.13459.

Ladwig, R., Furusato, E., Kirillin, G., Hinkelmann, R., Hupfer, M., 2018. Climate change demands adaptive management of urban lakes: model-based assessment of management scenarios for Lake Tegel (Berlin, Germany). Water 10, 186. https://doi.org/10.3390/w10020186.

Lenderink, G., Buishand, A., Van Deursen, W., 2007. Estimates of future discharges of the river Rhine using two scenario methodologies: direct versus delta approach. Hydrol. Earth Syst. Sci. 11, 1145–1159. https://doi.org/10.5194/hess-11-1145-2007.

Lenhart, T., Eckhardt, K., Fohrer, N., Frede, H.G., 2002. Comparison of two different approaches of sensitivity analysis. Phys. Chem. Earth 27, 645–654. https://doi.org/10.1016/S1474-7065(02)00049-9.

Lewis, W.M., 2000. Basis for the protection and management of tropical lakes. Lakes Reserv. Res. Manag. 5, 35–48. https://doi.org/10.1046/j.1440-1770.2000.00091.x.

Li, D., Feng, J., Xu, Z., Yin, B., Shi, H., Qi, J., 2019. Statistical bias correction for simulated wind speeds over CORDEX-East Asia. Earth Sp. Sci. 6, 200–211. https://doi.org/10.1029/2018EA000493.

Lopes, J.E.G., Braga, B.P.F., 1982. SMAP: A simplified hydrologic model. Applied Modeling in Catchment Hydrology. Water Resources Publications, Littleton, Co, pp. 167–176.

Magee, M.R., Wu, C.H., 2017. Response of water temperatures and stratification to changing climate in three lakes with different morphometry. Hydrol. Earth Syst. Sci. 21, 6253–6274. https://doi.org/10.5194/hess-21-6253-2017.

Mantzouki, E., Lürling, M., Fastner, J., de Senerpont Domis, L., Wilk-Wo'zniak, E., Koreivienė, J., Seelen, L., Teurlincx, S., Verstijnen, Y., Krztoń, W., Walusiak, E., Karosienė, J., Kasperovičienė, J., Savadova, K., Vitonytė, I., Cillero-Castro, C., Budzyńska, A., Goldyn, R., Kozak, A., Rosińska, J., Szeląg-Wasielewska, E., Domek, P., Jakubowska-Krepska, N., Kwasizur, K., Messyasz, B., Pełechata, A., Pełechaty, M., Kokocinski, M., García-Murcia, A., Real, M., Romans, E., Noguero-Ribes, J., Duque, D., Fernández-Morán, E., Karakaya, N., Häggqvist, K., Demir, N., Beklioğlu, M., Filiz, N., Levi, E., Iskin, U., Bezirci, G., Tavşanoğlu, Ü., Özhan, K., Gkelis, S., Panou, M., Fakioglu, Ö., Avagianos, C., Kaloudis, T., Çelik, K., Yilmaz, M., Marcé, R., Catalán, N., Bravo, A., Buck, M., Colom-Montero, W., Mustonen, K., Pierson, D., Yang, Y., Raposeiro, P., Gonçalves, V., Antoniou, M., Tsiarta, N., McCarthy, V., Perello, V., Feldmann, T., Laas, A., Panksep, K., Tuvikene, L., Gagala, I., Mankiewicz-Boczek, J., Yağcı, M., Çınar, Ş., Çapkın, K., Yağcı, A., Cesur, M., Bilgin, F., Bulut, C., Uysal, R., Obertegger, U., Boscaini, A., Flaim, G., Salmaso, N., Cerasino, L., Richardson, J., Visser, P., Verspagen, J., Karan, T., Soylu, E., Maraşlıoğlu, F., Napiórkowska-Krzebietke, A., Ochocka, A., Pasztaleniec, A., Antão-Geraldes, A., Vasconcelos, V., Morais, J., Vale, M., Köker, L., Akçaalan, R., Albay, M., Maronić, D.Š., Stević, F., Pfeiffer, T.Ž., Fonvielle, J., Straile, D., Rothhaupt, K.-O., Hansson, L.-A., Urrutia-Cordero, P., Bláha, L., Gerišˇ, R., Fránková, M., Koçer, M., Alp, M., Remec-Rekar, S., Elersek, T., Triantis, T., Zervou, S.-K., Hiskia, A., Haande, S., Skjelbred, B., Madrecka, B., Nemova, H., Drastichova, I., Chomova, L., Edwards, C., Sevindik, T., Tunca, H., Önem, B., Aleksovski, B., Krstić, S., Vucelić, I., Nawrocka, L., Salmi, P., Machado-Vieira, D., Oliveira, A. de, Delgado-Martín, J., García, D., Cereijo, J., Gomà, J., Trapote, M., Vegas-Vilarrúbia, T., Obrador, B., Grabowska, M., Karpowicz, M., Chmura, D., Úbeda, B., Gálvez, J., Özen, A., Christoffersen, K., Warming, T., Kobos, J., Mazur-Marzec, H., Pérez-Martínez, C., Ramos-Rodríguez, E., Arvola, L., Alcaraz-Párraga, P., Toporowska, M., Pawlik-Skowronska, B., Niedźwiecki, M., Pęczuła, W., Leira, M., Hernández, A., Moreno-Ostos, E., Blanco, J., Rodríguez, V., Montes-Pérez, J., Palomino, R., Rodríguez-Pérez, E., Carballeira, R., Camacho, A., Picazo, A., Rochera, C., Santamans, A., Ferriol, C., Romo, S., Soria, J., Dunalska, J., Sieńska, J., Szymański, D., Kruk, M., Kostrzewska-Szlakowska, I., Jasser, I., Žutinić, P., Udovič, M.G., Plenković-Moraj, A., Frąk, M., Bańkowska-Sobczak, A., Wasilewicz, M., Özkan, K., Maliaka, V., Kangro, K., Grossart, H.-P., Paerl, H., Carey, C., Ibelings, B., Mantzouki, E., Lürling, M., Fastner, J., de Senerpont Domis, L., Wilk-Woźniak, E., Koreivienė, J., Seelen, L., Teurlincx, S., Verstijnen, Y., Krztoń, W., Walusiak, E., Karosienė, J., Kasperovičienė, J., Savadova, K., Vitonytė, I., Cillero-Castro, C., Budzyńska, A., Goldyn, R., Kozak, A., Rosińska, J., Szeląg-Wasielewska, E., Domek, P., Jakubowska-Krepska, N., Kwasizur, K., Messyasz, B., Pełechata, A., Pełechaty, M., Kokocinski, M., García-Murcia, A., Real, M., Romans, E., Noguero-Ribes, J., Duque, D.P., Fernández-Morán, E., Karakaya, N., Häggqvist, K., Demir, N., Beklioğlu, M., Filiz, N., Levi, E.E., Iskin, U., Bezirci, G., Tavşanoğlu, Ü.N., Özhan, K., Gkelis, S., Panou, M., Fakioglu, Ö., Avagianos, C., Kaloudis, T., Çelik, K., Yilmaz, M., Marcé, R., Catalán, N., Bravo, A.G., Buck, M., Colom-Montero, W., Mustonen, K., Pierson, D., Yang, Y., Raposeiro, P.M., Gonçalves, V., Antoniou, M.G., Tsiarta, N., McCarthy, V., Perello, V.C., Feldmann, T., Laas, A., Panksep, K., Tuvikene, L., Gagala, I., Mankiewicz-Boczek, J., Yağcı, M.A., Çınar, Ş., Çapkın, K., Yağcı, A., Cesur, M., Bilgin, F., Bulut, C., Uysal, R., Obertegger, U., Boscaini, A., Flaim, G., Salmaso, N., Cerasino, L., Richardson, J., Visser, P.M., Verspagen, J.M.H., Karan, T., Soylu, E.N., Maraşlıoğlu, F., Napiórkowska-Krzebietke, A., Ochocka, A., Pasztaleniec, A., Antão-Geraldes, A.M., Vasconcelos, V., Morais, J., Vale, M., Köker, L., Akçaalan, R., Albay, M., Špoljarić Maronić, D., Stević, F., Žuna Pfeiffer, T., Fonvielle, J., Straile, D., Rothhaupt, K.-O., Hansson, L.-A., Urrutia-Cordero, P., Bláha, L., Gerišˇ, R., Fránková, M., Koçer, M.A.T., Alp, M.T., Remec-Rekar, S., Elersek, T., Triantis, T., Zervou, S.-K., Hiskia, A., Haande, S., Skjelbred, B., Madrecka, B., Nemova, H., Drastichova, I., Chomova, L., Edwards, C., Sevindik, T.O., Tunca, H., Önem, B., Aleksovski, B., Krstić, S., Vucelić, I.B., Nawrocka, L., Salmi, P., Machado-Vieira, D., de Oliveira, A.G., Delgado-Martín, J., García, D., Cereijo, J.L., Gomà, J., Trapote, M.C., Vegas-Vilarrúbia, T., Obrador, B., Grabowska, M., Karpowicz, M., Chmura, D., Úbeda, B., Gálvez, J.Á., Özen, A., Christoffersen, K.S., Warming, T.P., Kobos, J., Mazur-Marzec, H., Pérez-Martínez, C., Ramos-Rodríguez, E., Arvola, L., Alcaraz-Párraga, P., Toporowska, M., Pawlik-Skowronska, B., Niedźwiecki, M., Pęczuła, W., Leira, M., Hernández, A., Moreno-Ostos, E., Blanco, J.M., Rodríguez, V., Montes-Pérez, J.J., Palomino, R.L., Rodríguez-Pérez, E., Carballeira, R., Camacho, A., Picazo, A., Rochera, C., Santamans, A.C., Ferriol, C., Romo, S., Soria, J.M., Dunalska, J., Sieńska, J., Szymański, D., Kruk, M., Kostrzewska-Szlakowska, I., Jasser, I., Žutinić, P., Gligora Udovič, M., Plenković-Moraj, A., Frąk, M., Bańkowska-Sobczak, A., Wasilewicz, M., Özkan, K., Maliaka, V., Kangro, K., Grossart, H.-P., Paerl, H.W., Carey, C.C., Ibelings, B.W., 2018. Temperature effects explain continental scale distribution of cyanobacterial toxins. Toxins (Basel) 10, 156. https://doi.org/10.3390/toxins10040156.

Mi, C., Shatwell, T., Ma, J., Xu, Y., Su, F., Rinke, K., 2020. Ensemble warming projections in Germany's largest drinking water reservoir and potential adaptation strategies. Sci. Total Environ. 748, 141366. https://doi.org/10.1016/j.scitotenv.2020.141366.

Moe, S.J., Haande, S., Couture, R.-M., 2016. Climate change, cyanobacteria blooms and ecological status of lakes: a Bayesian network approach. Ecol. Model. 337, 330–347. https://doi.org/10.1016/j.ecolmodel.2016.07.004.

Moriasi, D.N., Arnold, J.G., Van Liew, M.W., Bingner, R.L., Harmel, R.D., Veith, T.L., 1983. Model evaluation guidelines for systematic quantification of accuracy in watershed simulations. Trans. ASABE 50 (3), 885–900 (ISSN 0001−2351).

Niedrist, G.H., Psenner, R., Sommaruga, R., 2018. Climate warming increases vertical and seasonal water temperature differences and inter-annual variability in a mountain lake. Clim. Chang. 151, 473–490. https://doi.org/10.1007/s10584-018-2328-6.

O'Reilly, C.M., Sharma, S., Gray, D.K., Hampton, S.E., Read, J.S., Rowley, R.J., Schneider, P., Lenters, J.D., McIntyre, P.B., Kraemer, B.M., Weyhenmeyer, G.A., Straile, D., Dong, B., Adrian, R., Allan, M.G., Anneville, O., Arvola, L., Austin, J., Bailey, J.L., Baron, J.S., Brookes, J.D., de Eyto, E., Dokulil, M.T., Hamilton, D.P., Havens, K., Hetherington, A.L., Higgins, S.N., Hook, S., Izmest'eva, L.R., Joehnk, K.D., Kangur, K., Kasprzak, P., Kumagai, M., Kuusisto, E., Leshkevich, G., Livingstone, D.M., MacIntyre, S., May, L., Melack, J.M., Mueller-Navarra, D.C., Naumenko, M., Noges, P., Noges, T., North, R.P., Plisnier, P.-D., Rigosi, A., Rimmer, A., Rogora, M., Rudstam, L.G., Rusak, J.A., Salmaso, N., Samal, N.R., Schindler, D.E., Schladow, S.G., Schmid, M., Schmidt, S.R., Silow, E., Soylu, M.E., Teubner, K., Verburg, P., Voutilainen, A., Watkinson, A., Williamson, C.E., Zhang, G., 2015. Rapid and highly variable warming of lake surface waters around the globe. Geophys. Res. Lett. 42, 10,773–10,781. https://doi.org/10.1002/2015GL066235.

Pilla, R.M., Williamson, C.E., Zhang, J., Smyth, R.L., Lenters, J.D., Brentrup, J.A., Knoll, L.B., Fisher, T.J., 2018. Browning-related decreases in water transparency lead to long-term increases in surface water temperature and thermal stratification in two small lakes. J. Geophys. Res. Biogeosci. 123, 1651–1665. https://doi.org/10.1029/2017JG004321.

Prats, J., Salençon, M.-J., Gant, M., Danis, P.-A., 2018. Simulation of the hydrodynamic behaviour of a Mediterranean reservoir under different climate change and management scenarios. J. Limnol. 77, 62–81.

Rathjens, H., Bieger, K., Srinivasan, R., Arnold, J.G., 2016. CMhyd User Manual - Documentation for Preparing Simulated Climate Change Data for Hydrologic Impact Studies.

Read, J.S., Hamilton, D.P., Jones, I.D., Muraoka, K., Winslow, L.A., Kroiss, R., Wu, C.H., Gaiser, E., 2011. Derivation of lake mixing and stratification indices from high-resolution lake buoy data. Environ. Model. Softw. 26, 1325–1336. https://doi.org/10.1016/j.envsoft.2011.05.006.

Read, J.S., Gries, C., Read, E.K., Klug, J., Hanson, P., Hipsey, M.R., Jennings, E., O'Reilly, C.M., Winslow, L.A., Pierson, D., McBride, C., Hamilton, D., 2016. Generating community-built tools for data sharing and analysis in environmental networks. Inl. Waters 6, 637–644. https://doi.org/10.5268/IW-6.4.889.

Reichstein, M., Bahn, M., Ciais, P., Frank, D., Mahecha, M.D., Seneviratne, S.I., Zscheischler, J., Beer, C., Buchmann, N., Frank, D.C., Papale, D., Rammig, A., Smith, P., Thonicke, K., Van Der Velde, M., Vicca, S., Walz, A., Wattenbach, M., 2013. Climate extremes and the carbon cycle. Nature. https://doi.org/10.1038/nature12350.

Ryu, I., Yu, S., Chung, S., 2020. Characterizing density flow regimes of three rivers with different physicochemical properties in a run-of-the-river reservoir. Water 12, 717. https://doi.org/10.3390/w12030717.

Sahoo, G.B., Forrest, A.L., Schladow, S.G., Reuter, J.E., Coats, R., Dettinger, M., 2016. Climate change impacts on lake thermal dynamics and ecosystem vulnerabilities. Limnol. Oceanogr. 61, 496–507. https://doi.org/10.1002/lno.10228.

Schwalm, C.R., Glendon, S., Duff, P.B., 2020. RCP8.5 tracks cumulative CO_2 emissions. Proc. Natl. Acad. Sci. U. S. A. 117 (33), 19656–19657. https://doi.org/10.1073/pnas.2007117117.

Shatwell, T., Thiery, W., Kirillin, G., 2019. Future projections of temperature and mixing regime of European temperate lakes. Hydrol. Earth Syst. Sci. 23. https://doi.org/10.5194/hess-23-1533-2019.

da Silva, F. das N.R., Alves, J.L.D., Cataldi, M., 2019. Climate downscaling over South America for 1971–2000: application in SMAP rainfall-runoff model for Grande River Basin. Clim. Dyn. 52, 681–696. https://doi.org/10.1007/s00382-018-4166-7.

Soares, L.M.V., Silva, T.F.G., Vinçon-Leite, B., Eleutério, J.C., De Lima, L.C., Nascimento, N.O., 2019. Modelling drought impacts on the hydrodynamics of a tropical water supply reservoir Modelling drought impacts on the hydrodynamics of a tropical water supply reservoir. Inl. Waters https://doi.org/10.1080/20442041.2019.1596015.

Soil Conservation Service – (SCS), 1964. Estimation of direct runoff from storm rainfall. National Engineering Handbook. Section 4 – Hydrology. Chapter 10. Hydraulic Engineer (30p.).

Taniwaki, R.H., Rosa, A.H., Lima, R. De, Maruyama, C.R., Secchin, L.F., Calijuri, M. do C., Moschini-Carlos, V., 2013. A influência do uso e ocupação do solo na qualidade e genotoxicidade da água no Reservatório de Itupararanga, São Paulo, Brasil. Interciencia 38, 164–170.

Teutschbein, C., Seibert, J., 2012. Bias correction of regional climate model simulations for hydrological climate-change impact studies: review and evaluation of different methods. J. Hydrol. 456–457, 12–29. https://doi.org/10.1016/j.jhydrol.2012.05.052.

TOPODATA, 2020. Brazil geomorphometric database. http://www.dsr.inpe.br/topodata/dados.php. (Accessed 18 January 2020).

Tundisi, J.G., Matsumura Tundisi, T., Tundisi, J., Blanco, F., Abe, D.S., Contri Campanelli, L., Sidagis Galli, G., Silva, V., Lima, C., 2015. A bloom of cyanobacteria (*Cylindrospermopsis raciborskii*) in UHE Carlos Botelho (Lobo/Broa) reservoir: a consequence of global change? Braz. J. Biol. 75, 507–508. https://doi.org/10.1590/1519-6984.24914.

Vargas, S.R., dos Santos, P.V., Bottino, F., Calijuri, M. do C., 2020. Effect of nutrient concentration on growth and saxitoxin production of Raphidiopsis raciborskii (Cyanophyta) interacting with *Monoraphidium contortum* (Chlorophyceae). J. Appl. Phycol. 32, 421–430. https://doi.org/10.1007/s10811-019-01972-w.

Wells, M.L., Trainer, V.L., Smayda, T.J., Karlson, B.S.O., Trick, C.G., Kudela, R.M., Ishikawa, A., Bernard, S., Wulff, A., Anderson, D.M., Cochlan, W.P., 2015. Harmful algal blooms and climate change: learning from the past and present to forecast the future. Harmful Algae 49, 68–93. https://doi.org/10.1016/j.hal.2015.07.009.

Woolway, R.I., Merchant, C.J., 2019. Worldwide alteration of lake mixing regimes in response to climate change. Nat. Geosci. 12, 271–276. https://doi.org/10.1038/s415610190322x.

Woolway, R.I., Weyhenmeyer, G.A., Schmid, M., Dokulil, M.T., De Eyto, E., Maberly, S.C., May, L., Merchant, C.J., 2019. Substantial increase in minimum lake surface temperatures under climate change. Clim. Chang. 155, 81–94. https://doi.org/10.1007/s10584-019-02465-y.

Woolway, R.I., Kraemer, B.M., Lenters, J.D., Merchant, C.J., O'Reilly, C.M., Sharma, S., 2020. Global lake responses to climate change. Nat. Rev. Earth Environ., 1–16 https://doi.org/10.1038/s43017-020-0067-5.

Zhang, X., Wang, K., Frassl, M.A., Boehrer, B., 2020. Reconstructing six decades of surface temperatures at a shallow lake. Water 12, 405. https://doi.org/10.3390/w12020405.